

EVALUATING VISCOUS POTENTIAL FUNCTION FOR RATE SENSITIVITY IN SOFT MATERIALS

Stephen Melly¹, Aleksander Czekanski^{1*},

¹Department of Mechanical Engineering, Lassonde School of Engineering, York University, Toronto, Canada
 *alex.czekanski@lassonde.yorku.ca

Abstract—Strain rate sensitivity plays a vital role in numerically modeling the mechanical behavior of soft materials, especially in applications such as biomechanics, polymer engineering, and soft robotics. This study examines a viscous potential function proposed by Upadhyay et al. (2020) to model strain rate sensitivity in soft materials. The function is evaluated for its ability to capture experimentally observed rate-dependent behavior using data from the literature on polyvinyl alcohol (PVA) hydrogel and self-healing hydrogel. The predictive performance of the model is assessed using the coefficient of determination. The results indicate that the viscous potential function, incorporating both linear and nonlinear rate sensitivity parameters, offers improved accuracy and broad applicability to a range of soft materials.

Keywords—Viscous potential function; strain rate sensitivity; soft materials; viscoelasticity

I. INTRODUCTION

The mechanical response of soft materials, such as hydrogels, elastomers, and biological tissues, is heavily influenced by their strain rate sensitivity, a key factor in applications spanning biomechanics and flexible electronics. Experimental observations show that the stress-strain curves of soft materials undergo significant variations as strain rates increase from quasi-static to dynamic ranges. This direct relationship between strain rate and stress-strain curve serves as a guiding principle for developing mathematical models to predict mechanical behavior [7].

Two primary formulations, integral-type and differential-type, are commonly used to model rate sensitivity in soft materials [1]. Integral-type formulations account for stress relaxation through exponential decay in their functional expressions but do not directly incorporate the rate of deformation. Consequently, additional stress relaxation experiments are required to characterize the material's time-dependent response [7]. Differential-type formulations derive stress from a Helmholtz free energy function, which incorporates the deformation history to account for strain rate sensitivity [1]. This approach eliminates the need for stress relaxation experiments, relying

solely on stress-strain responses at various strain rates.

Pioletti et al. [2] introduced an energy-based approach in which the energy expression is divided into elastic and viscous components. The viscous potential is defined as a function of the Right Cauchy-Green deformation tensor, \mathbf{C} , and its first time derivative, $\dot{\mathbf{C}}$. This framework provides significant advantages compared to other modeling approaches [1], [5] and has been utilized to simulate rate-dependent behavior of various soft materials, including semilunar heart valves [8], skeletal muscle tissues [10], liver tissue [11], synthetic tissues [9], and aortic heart valves [7]. Researchers have proposed various new forms of viscous potentials over time [5], [11]. Upadhyay et al. [5] demonstrated that their proposed viscous potential improves fitting accuracy while mitigating potential thermodynamic instabilities in quasi-static hyperelastic models affecting the dynamic response. In this study, we further assess the model's applicability to a diverse range of soft materials by using it to predict the strain rate-dependent behavior of PVA hydrogel and self-healing hydrogel.

II. CONSTITUTIVE MODEL

A. Energy Potential

The total strain energy density comprises the elastic and viscous potentials. We assume that the material is slightly compressible, therefore, the strain energy density is expressed as a decoupled sum of isochoric and volumetric components. The isochoric part of elastic potential, Ψ_e^{iso} , follows the formulation proposed by Yeoh [3], while the volumetric component is derived from [4]. The form of viscous component, Ψ_v^{iso} , was proposed by Upadhyay et al. [5] (1).

$$\begin{aligned}\Psi_e^{\text{iso}} &= c_{10} (I_1^* - 3) + c_{20} (I_1^* - 3)^2 + c_{30} (I_1^* - 3)^3 \\ \Psi^{\text{vol}} &= \frac{k}{4} (J^2 - 2 \ln J - 1) \\ \Psi_v^{\text{iso}} &= k_{11} \sqrt{I_1^* - 3} J_2^* + k_{21} \sqrt{I_2^* - 3} J_5^{*c_{21}}\end{aligned}\quad (1)$$

Where $c_{10}, c_{20}, c_{30}, k_{11}, k_{21}$, and c_{21} are material parameters that are determined using optimization techniques, while k denotes the bulk modulus, which is calculated based on its relationship with Poisson's ratio and the shear modulus. Given the distortional components, $\mathbf{C}^* = J^{-2/3} \mathbf{F}^\top \mathbf{F}$ and $\dot{\mathbf{C}}^* = J^{-2/3} (\dot{\mathbf{F}}^\top \mathbf{F} + \mathbf{F}^\top \dot{\mathbf{F}})$, the invariants are obtained as (2).

$$\begin{aligned} I_1^* &= \text{tr}[\mathbf{C}^*] \quad I_2^* = \frac{1}{2} [(I_1^*)^2 - \text{tr}(\mathbf{C}^*)^2] \\ J_2^* &= \text{tr}[\dot{\mathbf{C}}^{*2}], \quad J_5^* = \text{tr}(\mathbf{C}^* \dot{\mathbf{C}}^{*2}) \end{aligned} \quad (2)$$

B. Stress Tensor

The total stress is obtained by summing the contributions from volumetric and isochoric (for both the elastic and viscous parts) (3).

$$\begin{aligned} \mathbf{S} &= \mathbf{S}_e^{\text{iso}} + \mathbf{S}_{\text{vol}} + \mathbf{S}_v^{\text{iso}} \\ \mathbf{S} &= 2 \left[\frac{\partial \Psi_e^{\text{iso}}}{\mathbf{C}} + \frac{\partial \Psi_v^{\text{vol}}}{\mathbf{C}} + \frac{\partial \Psi_v^{\text{iso}}}{\dot{\mathbf{C}}} \right] \end{aligned} \quad (3)$$

By using (1) in (3), the resulting expressions for stress take the following form (4).

$$\begin{aligned} \mathbf{S}_{\text{vol}} &= \frac{Jk}{2} \left(J - \frac{1}{J} \right) \mathbf{C}^{-1} \\ \mathbf{S}_v^* &= 4k_{11} \left(\sqrt{I_1^*} - 3 \right) \dot{\mathbf{C}}^* + \\ &\quad 2 \frac{c_{21} k_{21}}{J_5^*} J_5^{*c_{21}} \left(\sqrt{I_2^*} - 3 \right) \mathbf{C}^* \dot{\mathbf{C}}^* + \dot{\mathbf{C}}^* \mathbf{C}^* \\ \mathbf{S}_e^* &= 2 \left[c_{10} + 2c_{20} (I_1^* - 3) + 3c_{30} (I_1^* - 3)^2 \right] \mathbf{I} \\ \mathbf{S}_{\text{iso}} &= J^{-\frac{2}{3}} \text{Dev}(\mathbf{S}_v^* + \mathbf{S}_e^*) \\ \mathbf{S} &= \mathbf{S}_{\text{vol}} + \mathbf{S}_{\text{iso}} \end{aligned} \quad (4)$$

The Cauchy stress tensor is then obtained via a push-forward operation $\boldsymbol{\sigma} = J^{-1} \mathbf{F} \mathbf{S} \mathbf{F}^\top$.

III. PARAMETER DETERMINATION

The model requires six parameters: three for the elastic component and three for the viscous component. We defined an objective function as the sum of squared errors, representing the total squared difference between the predicted and experimental values. To minimize this error, we employed Python's `scipy.optimize.minimize` function, using the Nelder-Mead algorithm.

The elastic parameters were determined using the stress-stretch data obtained at the lowest strain rate, which was assumed to represent quasi-static conditions: 0.001 s^{-1} for PVA hydrogel and 0.003 s^{-1} for self-healing hydrogel. The viscous parameters were subsequently determined using simultaneous data at higher strain rates. The elastic parameters for both materials are shown in Table I.

The optimized viscous parameters for each material are shown in Table II.

TABLE. I
ELASTIC PARAMETERS

Material	c_{10}	c_{20}	c_{30}
PVA hydrogel	13386.2021	-0.01	337.7422
Self-healing hydrogel	2211.6371	-355.4243	71.2467

TABLE. II
VISCIOUS PARAMETERS

Material	k_{11}	k_{21}	c_{21}
PVA hydrogel	6.8625	2683.3916	0.5755
Self-healing hydrogel	15169.4583	-4407.0087	1.0097

IV. RESULTS

The model accurately captured the rate-dependent behavior of PVA hydrogel, achieving coefficients of determination, R^2 , greater than 0.99, as shown in Fig. 1. The model is versatile enough to capture the a wide range of rate-sensitivity, accommodating strain rates from quasi-static to dynamic.

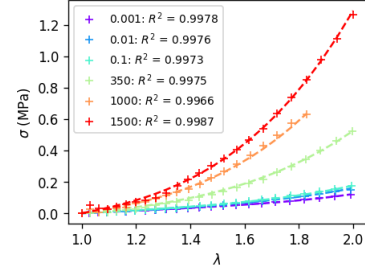


Figure. 1. Comparison of the experimental and predicted stress-stretch curves for PVA hydrogel. Symbols represent experimental data, while dashed lines indicate model predictions

The predictions for the self-healing hydrogel demonstrated acceptable accuracy, though the accuracy decreased with increasing strain rates, as illustrated in Fig. 2.

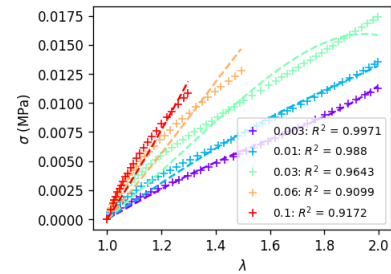


Figure. 2. Comparison of the experimental and predicted stress-stretch curves for self-healing hydrogel. Symbols represent experimental data, while dashed lines indicate model predictions

V. CONCLUSION

The assessment of the viscous potential offered valuable insights into its capability to capture the rate-dependent behavior of soft materials, particularly hydrogels. The accuracy of the model is influenced by the characteristics of the stress-stretch

curves. For PVA hydrogels, which display standard S-shaped curves, the model demonstrated higher accuracy. In contrast, the self-healing hydrogel, with its distinct curve shape, resulted in reduced accuracy. The results demonstrate that the viscous potential explored in this study is versatile and applicable to a wide variety of materials with commendable accuracy.

ACKNOWLEDGMENT

We acknowledge the support of the Natural Sciences and Engineering Research Council of Canada (NSERC).

Nous remercions le Conseil de recherches en sciences naturelles et en génie du Canada (CRSNG) de son soutien.



Natural Sciences and Engineering
Research Council of Canada

Conseil de recherches en sciences
naturelles et en génie du Canada



REFERENCES

- [1] Ahsanizadeh, S. and L. Li, "Visco-hyperelastic constitutive modeling of soft tissues based on short and long-term internal variables", *BioMedical Engineering OnLine*, vol. 14, no. 1, pp. 29, 2015.
- [2] D. P. Pioletti, L. R. Rakotomanana, J.-F. Benvenuti, and P.-F. Leyvraz, "Viscoelastic constitutive law in large deformations: application to human knee ligaments and tendons," *Journal of Biomechanics*, vol. 31, no. 8, pp. 753–757, 1998.
- [3] O. H. Yeoh, "Characterization of Elastic Properties of Carbon-Black-Filled Rubber Vulcanizates," *Rubber Chemistry and Technology*, vol. 63, no. 5, pp. 792–805, 1990.
- [4] G. A. Holzapfel, *Nonlinear Solid Mechanics: A Continuum Approach for Engineering*, John Wiley & Sons, 2000.
- [5] K. Upadhyay, G. Subhash, and D. Spearot, "Visco-hyperelastic constitutive modeling of strain rate sensitive soft materials," *Journal of the Mechanics and Physics of Solids*, vol. 135, p. 103777, 2020.
- [6] R. Long, K. Mayumi, C. Creton, T. Narita, and C.-Y. Hui, "Time Dependent Behavior of a Dual Cross-Link Self-Healing Gel: Theory and Experiments," *Macromolecules*, vol. 47, no. 20, pp. 7243-7250, 2014.
- [7] Afshin Anssari-Benam, Yuan-Tsan Tseng, Martino Pani, and Andrea Bucchi, "Modelling the rate-dependency of the mechanical behaviour of the aortic heart valve: An experimentally guided theoretical framework," *Journal of the Mechanical Behavior of Biomedical Materials*, vol. 134, pp. 105341, 2022.
- [8] Afshin Anssari-Benam, Yuan-Tsan Tseng, Martino Pani, and Andrea Bucchi, "A New Dissipation Function to Model the Rate-Dependent Mechanical Behavior of Semilunar Valve Leaflets," *Journal of Biomechanical Engineering*, vol. 145, no. 7, pp. 071004, 2023.
- [9] Zahra Matin Ghahfarokhi, Mahdi Moghimi Zand, Mehdi Salmani Tehrani, Brianna Regina Wendland, and Roozbeh Dargazany, "A visco-hyperelastic constitutive model of short- and long-term viscous effects on isotropic soft tissues," *Proceedings of the Institution of Mechanical Engineers, Part C: Journal of Mechanical Engineering Science*, vol. 234, no. 1, pp. 3-17, 2020.
- [10] Y.T. Lu, H.X. Zhu, S. Richmond, and J. Middleton, "A visco-hyperelastic model for skeletal muscle tissue under high strain rates," *Journal of Biomechanics*, vol. 43, no. 13, pp. 2629-2632, 2010.
- [11] Zahra Matin Ghahfarokhi, Mehdi Salmani-Tehrani, Mahdi Moghimi Zand, and Sara Esmailian, "A New Viscous Potential Function for Developing the Viscohyperelastic Constitutive Model for Bovine Liver Tissue: Continuum Formulation and Finite Element Implementation," *International Journal of Applied Mechanics*, vol. 12, no. 3, pp. 2050029, 2020.